NOTES

Terrestrial heat flow in Junggar Basin, Northwest China

WANG Shejiao[1,2], HU Shengbiao[1], LI Tiejun[1], WANG Jiyang[1] & ZHAO Wenzhi[2]

1. Institute of Geology and Geophysics, Chinese Academy of Sciences, Beijing 100029, China;
2. Research Institute of Petroleum Exploration and Development, CNPC, Beijing 100083, China

Abstract Based on temperature logs of 117 boreholes and thermal conductivity of 119 rock samples, the first group of 35 heat flow data in the Junggar Basin are presented. The thermal gradients vary between 11.6 and 26.5℃/km , and the thermal conductivity changes from 0.17 to 3.6 W/mK. Heat flow ranges from 23.4 to 53.7 mW/m^2 with a mean of (42.3±7.7) mW/m^2. The heat flow pattern shows that heat flow is higher in the uplifts and lower in the depressions. The factors affecting the heat flow and its distribution include basin type, basement structure, sediment thickness, radioactive heat generation, etc. The overall low present-day heat flow in the Junggar Basin reflected its tectonothermal evolution characterized by lithospheric thickening, thrust and fault at shallow crust as well as consequently quick subsidence during the Late Cenozoic.

Keywords: geothermal gradient, thermal conductivity, terrestrial heat flow, Junggar Basin.

The Junggar Basin, one of the three large basins in the Xinjiang region, is located in the north part of the Xinjiang Uygur Autonomous Region, Northwest China. It is bounded on the south by the Tianshan Mountains and on the east by the Kelameili Mountains and on the northwest by the Zhayier Mountains. The Junggar Basin, like a triangle, covers an area of about 134 000 km^2.

The petroleum exploration in the Junggar Basin started 50 years ago. Up to now, 23 oil and gas fields have been discovered. In recent years, many reservoirs have been found in the southern and central parts of the basin. All these achievements show that the Junggar Basin has a prospect for petroleum exploration.

As an important aspect of basin analysis, thermal parameters, such as thermal gradient and heat flow, are crucial to modeling of the thermal maturation of oil-source rocks, and of the dynamic evolution of a basin. It is also of importance for trapping and sealing of potential oil reservoir formation as many geological processes, such as fluid overpressure, diagenesis of sediments, are temperature-dependent.

Based on 117 borehole temperature logs and 119 thermal conductivity data, including 90 newly measured and 29 collected data, 35 heat flow values were presented as the first group of heat flow data from the Junggar Basin. Furthermore, the tectonothermal implications of the present-day heat flow data are discussed.

1 Geological setting and heat flow sites

The Junggar Basin has two types of basement: the Precambrian crystallined basement and the deformed basement during the Hercynian Movement. The Junggar Basin is a typical superimposed compound basin at present due to its complex tectonic developments. The basin is composed of four uplifts, i.e. the Luliang, the Zhongyang, the Dongbu, and the Chepaizi uplifts, and three depressions including the Wulungu, the Zhongyang, and the Tianshan foreland depressions, and one overthrust belt (fig. 1).

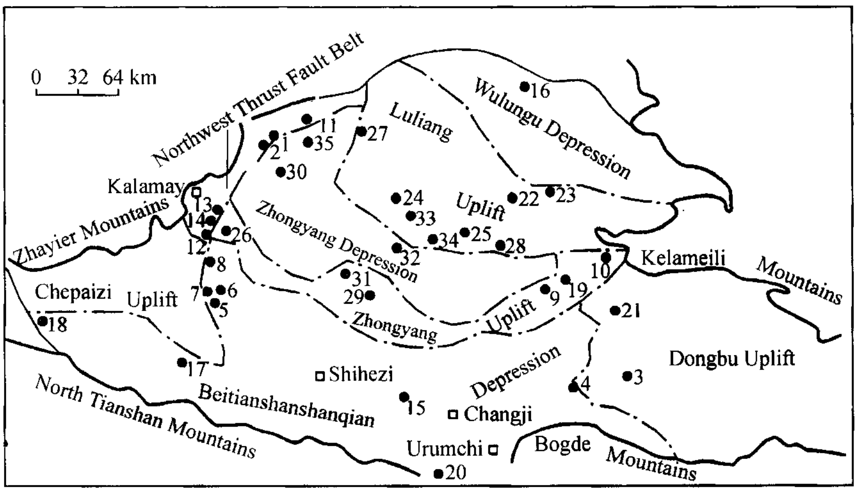

Fig. 1. Heat flow sites and tectonic setting (the site numbers correspond to those in table 2).

Generally, the petroleum exploration is concentrated on the uplifts, therefore, the distribution of drill holes is uneven. Most of them were located in the uplifts. A few of them were scattered in the depressions. For this reason, the heat flow sites are restricted by the borehole distribution.

2 Borehole temperature and thermal conductivity

Temperature logs from 117 boreholes have been analyzed. Most wells only logged temperature in part of the section, a few logged the whole section. The temperature profiles show that the temperatures with depth have quite different trends for different wells, which may result from groundwater convection or the equilibrium time between the rock wall and fluid is not enough to let the temperature recover its original condition. Only 28 wells were selected out for thermal gradient calculation (fig. 2). Additional BHT data of 8 drill holes were used to estimate the thermal gradient.

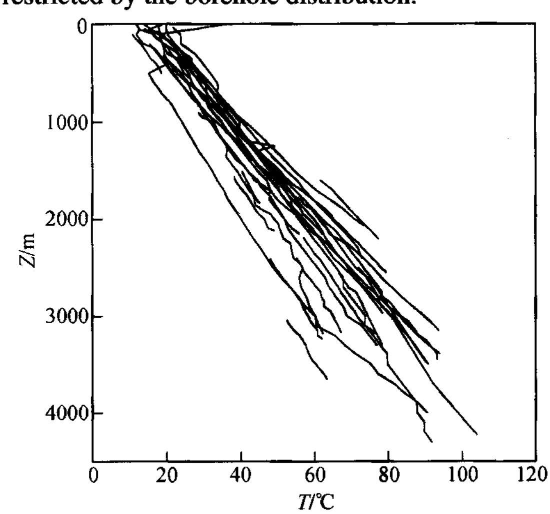

Fig. 2. Temperature profiles in heat flow calculation wells.

90 new thermal conductivity samples were measured using the ring heat source thermal

conductivity meter, and 28 conductivity data were collected from the former works. The rock samples almost covered all types of sedimentary rocks in the Junggar Basin, even the dolomite, limestone and volcanic were also included. All the thermal conductivity data and the lithology are summarized in table 1

Table 1 Measured thermal conductivity values in the Junggar Basin

Lithology	Formation	Thermal conductivity/W • m^{-1} • K^{-1}	Amount	Average (S. E.)
Mudstone		0.867—2.661	45	1.878 (0.38)
	N	1.722—1.871	3	
	E	0.867—1.349	2	
	K	1.763—2.004	5	
	J	1.152—2.382	13	
	T	1.282—2.661	8	
	P	1.248—2.344	12	
	C	1.846—2.232	2	
Siltstone		1.232—2.890	11	1.841 (0.54)
	N	1.842	1	
	E	1.232	1	
	K	1.299—1.571	3	
	J	1.366—2.890	3	
	P	2.107—2.414	3	
Sandstone		0.687—3.268	41	2.166 (0.69)
	N	0.856	1	
	E	0.796—1.908	2	
	K	1.109—1.187	2	
	J	0.972—3.268	22	
	T	2.813—2.909	3	
	P	0.687—2.837	11	
Conglomerate		2.061—3.345	5	2.585 (0.53)
	J	2.345	1	
	T	2.614	1	
	P	2.061—3.345	3	
Volcanic		1.665—2.557	14	1.976 (0.37)
	J	1.665—2.069	2	
	T	2.045—2.176	2	
	P	1.691—2.331	2	
	C	1.289—2.557	8	
Coal	J	0.169	1	0.169
Limestone	C	1.847	1	1.847
Dolomite	P	3.636	1	3.636

The measured thermal conductivity for sandstone is highly scattered relative to any other lithologies due to the differences in mineral composition and structure of the rocks. The relationship between thermal conductivity and the present-day burial depth for the same lithology is poor except for sandstone.

3 Heat flow calculation

Heat flow is a comprehensive parameter to reflect the regional thermal regime. The heat flow cannot be directly measured from subsurface but calculated by the gradient times the thermal conductivity. It is an indirect physical parameter and represents the component of the conductive heat flow. Thus, the accuracy of heat flow determination depends on the calculated gradient and the measured thermal conductivity. In order to decrease errors, thermal gradient data from the 28 selected wells are calculated. A thickness weighted method is used for the mean thermal conductivity calculation. The heat flow values for all the 28 wells together with the 8 estimated data are presented in table 2.

Table 2 Data of heat flow in the Junggar Basin

No.	Well No.	Longitude	Latitude	Range/m	Lithology	Gradient G±SD/ ℃ • km^{-1}	Gradient Coef.	Cond./ W • m^{-1} • K^{-1}	H.F. /mW • m^{-2}
1	Bai57	85°30′17″	45°59′20″	1 350—1 830	sandstone, conglomerate	18.5±0.12	0.998	2.0825	38.5
2	Bai6	85°29′14″	45°51′25″	260—2 150	mudstone, sandstone	20.3±0.06	0.999	2.0860	42.3
3	Bei21	88°48′08″	44°22′25″	100—2 430	mudstone	21.5±0.11	0.998	1.9825	42.6
4	Bei74	88°23′51″	44°14′28″	2 190—3 177	mudstone	18.5±0.08	0.996	1.9365	35.8
5	Che17	84°57′42″	44°44′42″	3 040—3 650	mudstone, sandstone	17.2±0.10	0.990	1.9290	33.2
6	Che2025	84°57′30″	45°51′25″	2 410—3 230	mudstone, sandstone	17.2±0.10	0.993	1.9036	32.7
7	Che2037	84°56′22″	44°46′16″	2 400—3 170	mudstone, sandstone	15.8±0.09	0.993	1.9116	30.2
8	Che30	84°52′59″	44°58′47″	30—2 970	mudstone, sandstone	20.3±0.05	1.000	1.9333	39.2
9	Cai31	88°12′51″	44°56′03″	1 800—3 390	mudstone, sandstone	26.9±0.10	0.999	1.9528	52.2
10	Caican1	88°48′16″	45°07′50″	700—3 154	vulcanite	26.0±0.14	0.999	2.0350	52.8
11	Cong43	85°48′28″	46°08′20″	100—495	sandstone	20.1±0.06	0.997	2.1660	43.5
12	Hong1	84°56′12″	45°12′14″	1 560—2 120	sandstone, mudstone	18.7±0.10	0.992	2.0367	38.1
13	Hong31	85°02′51″	45°23′44″	320—2 550	sandstone, mudstone	27.6±0.07	0.999	1.8926	52.3
14	Hong35	85°01′30″	45°20′48″	200—2 150	sandstone, mudstone	24.7±0.09	0.999	1.9795	48.9
15	Hu2	86°59′10″	44°10′40″	100—3 500	mudstone, siltstone	21.4±0.29	0.998	1.9827	42.4
16	Lun5	87°53′46″	46°20′00″	0—3 300	sandstone, conflomerate	19.5±0.17	0.998	2.2140	43.2
17	Xican2	84°41′15″	44°23′01″	500—4 000	mudstone, sandstone	20.5±0.22	0.997	1.8999	38.9
18	Sican1	84°09′00″	44°37′17″	35—4 300	mudstone	16.5±0.16	0.998	1.9982	33.0
19	Caican2	88°22′05″	45°51′25″	1 600—2 200	sandstone, mudstone	25.7±0.11	0.998	2.0220	52.0
20	Xiao1	87°18′20″	43°37′18″	2 600—3 180	mudstone, siltstone	11.6±0.10	0.992	2.0209	23.4
21	Sha'nan1	88°49′26″	44°45′54″	200—2 066	mudstone	27.1±0.28	0.995	1.9496	52.8
22	Sancan1	87°55′06″	45°35′13″	100—2 400	mudstone, siltstone	23.7±0.11	0.999	1.9438	46.1
23	Quan3	88°06′44″	45°37′11″	50—3 450	mudstone, siltstone	22.9±0.12	0.998	1.9384	44.4
24	Shinan4	86°44′04″	45°37′32″	2 566—3 302	sandstone	16.7±0.01	0.995	2.1191	35.4
25	Shinan2	87°33′49″	45°24′57″	2 506—4 230	mudstone	18.1±0.15	0.995	1.9896	35.9
26	Guai4	85°09′54″	45°14′35″	1 908—3 472	sandstone, mudstone	19.3±0.23	0.996	2.0670	39.9
27	Madong1	86°27′14″	46°07′00″	3 248—4 548	mudstone	26.5±0.35	1.000	1.9663	52.1
28	Dixi2	87°41′24″	45°11′47″	3 203—3 835	mudstone, sandstone	26.0±0.56	0.992	1.9646	51.1
29	Pencan2*	86°31′26″	44°54′55″	0—5 180	sandstone, mudstone	20.9		2.0076	42.0
30	Aican1*	85°39′25″	45°46′43″	0—5 300	mudstone, sandstone	18.7		2.0236	37.8
31	Pen4*	86°18′32″	45°03′02″	0—4 265.6	sandstone, mudstone	20.4		2.0076	41.0
32	Mobei2*	86°44′23″	45°13′40″	0—4 438	mudstone, sandstone	23.2		1.9783	45.9
33	Shixi2*	86°53′12″	45°26′04″	0—4 578.5	sandstone, mudstone	26.2		2.0493	53.7
34	Lu'nan1*	87°08′52″	45°18′47″	0—4 349.9	mudstone, sandstone	26.2		2.0207	52.9
35	Ma2*	85°57′18″	45°57′51″	0—2 632.5	mudstone, sandstone	17.9		1.9956	35.7

* Thermal gradient calculated from BHT.

4 Heat flow distribution

Heat flow in the Junggar Basin ranges from 23.4 to 53.7 mW/m^2 with an average of 42.3 mW/m^2, lower than the mean value of (62.6 ± 24.2) mW/m^2 in the continent area of China. The heat flow pattern shows that heat flow is higher in the uplifts and lower in the depressions. The highest heat flow is distributed in the Luliang uplift with a mean value of (45.3 ± 7.9) mW/m^2, next in the Zhongyang uplift with mean value of (45.2 ± 5.7) mW/m^2. The mean heat flow in the northwestern overthrust belt and in the Dongbu uplift are 43.9 and 43.7 mW/m^2, respectively. In the Lun-5 Well in the Wulungu depression it is 43.2 mW/m^2, whereas it is 35.7 and 37.8 mW/m^2 respectively in the Ma-2 Well and the Aican-1 Well in the Zhongyang depression. An average heat flow in North Tianshan foreland depression is (34.4 ± 8.3) mW/m^2; the lowest one is observed in the Xiao-1 Well in which the heat flow value is only 23.4 mW/m^2.

It should be noted that the heat flow in the same tectonic unit has significant variation. For example, among the 8 measured heat flow data in the Luliang uplifts, the heat flow in Shinan-2 and Shinan-4 wells are 35.9 and 35.4 mW/m^2, respectively, obviously lower than others in the same unit. Analysis indicates that these two wells are located in a subtectonic units, the Shinan depression where the basements buried deeper and the geothermal gradients are consequently lower. The same observations can also be seen in other tectonic units.

Generally, the heat flow is controlled by the basement structure of the basin, the same situation is also observed in the Tarim Basin where the heat flow is slightly higher than in the Junggar Basin.

5 Factors affecting heat flow pattern

There are many factors that may affect the heat flow. The main factors in the Junggar Basin are analyzed as below:

(i) Type of sedimentary basin. Because the heat flow value is conductive heat flow, the type of sedimentary basins is often characterized by different characteristic heat flow. Heat flow is higher in young rift basin and back-arc basin with active volcanic activity, and lower in foreland and craton basins. The Junggar Basin has an old craton basement and was developed as foreland basin during the whole Cenozoic, so its heat flow should not be as high as observed. The lower heat flow in the Junggar Basin reflects its stable tectonothermal evolution during Mesozoic to Cenozoic.

(ii) Basement structure and sediment thickness. Heat flow is higher in the uplifts and lower in the depressions, which results from the heat refraction effect. The uplift with higher thermal conductivity due to shallow basement burial depth and thin sedimentary cover thickness would cause heat concentration toward it relative to the depressions. The depression is the sedimentary center where the mudstone is generally thick and its thermal conductivity is lower than other lithologies. The conductive heat flow from deeper crust are, therefore, redistributed to the higher thermal conductivity uplift. As a result, the heat flow in uplifts is higher than that in depressions.

Sedimentation can decrease the surface heat flow. The decreased amount is determined by the thermal conductivity, the deposition rate and the duration of sedimentation. The bigger the sediment rate, the more obviously the heat flow decreases. For example, the heat flow is 30—40 mW/m^2 in the south of the basin with high deposition rate and thickness, much lower than other areas. It results from the quick subsidence and huge thick sediments with lower thermal conductivity during Late Tertiary.

(iii) Radiogenic heat production. The radioactive heat generation in the sedimentary rocks has some influences on the surface heat flow. Through the conversion of the gamma ray values, the total radioactive heat contribution in the sediments to the surface heat flow can reach as much as about 10—18 mW/m^2, account for about 25% of the surface heat flow; therefore, the influence of radioactive heat generation on the sedments should not be ignored.

6 Implications of tectonothermal evolution

Terrestrial heat flow is an objective reflectance of the tectonothermal evolution of a basin. The thermal regime in different types of basin has significant differences. Rift basin, like the Nanhai Basin, the Baikal and the East-Africa rifts have higher heat flow. Craton basin, such as the Tarim Basin, the

Williston and the Michigan basins in North America, has lower heat flow. The Junggar Basin has a stable craton basement with a crustal thickness of 44—46 km. The shape of the top of the mantle shows that it is a triangle and tilts up to the north. The P-wave speed in lithosphere contains a low speed layer at about 34 km depth with a 9—10 km thickness. All these geophysical backgrounds determine the low thermal regime of the Junggar Basin at present.

The Junggar Basin experienced several dynamic evolution stages, including rifting during the Carboniferous-Permian, uplifting and subsiding in the Menozoic and a foreland basin in the Cenozoic. The heat flow pattern at present reflects the tectonic features of the Cenozoic foreland basin.

Tectonic subsidence analysis shows that the Junggar Basin subsided slowly in the Early Tertiary but quickly in the Late Tertiary. The quick subsidence caused by the collision between the Indian and the Eurasian plates resulted in the thickening of the lithosphere and tilted up towards the north. Huge thick sediment deposited in the Tianshan foreland region. The process is a cooling process and lowers the apparent surface heat flow. It can be distinguished from the rift during the Carboniferous-Permian that when the lithosphere was thinning although the quick subsidence accompanied it, it is a heating process.

The results presented by Turcotte et al.[7] show that the time of thermal relaxation for lithospheric scale is about 62 Ma, that is to say, the abnormal thermal disturbance caused by tectonothermal activity within lithosphere, like volcanic eruptions, will have no influences after 62 Ma. Although the Junggar Basin was a rift basin with volcanic activity and had higher heat flow during the Carboniferous-Permian, it cannot last to the present. The heat flow features at present only reflect the tectonothermal evolution characterized by lithospheric thickening, thrust and fault at shallow crust as well as consequently quick subsidence during the Late Cenozoic.

Acknowledgements This work was supported by the National Natural Science Foundation of China (Grant No. 49672169).

References

1. Wang Ji'an, Xiong Liangping, Yang Shuzhen, Geothermics and Petroleum (in Chinese), Beijing: Science Press, 1985, 15—25.
2. Hu Shengbiao, Xiong Liangping , Wang Jiyang et al., The first group of heat flow report in Jiangxi Province, Chinese Science Bulletin (in Chinese), 1992(19): 1791.
3. Carter, L. S., Kelley, S. A., Blackwell, D. D. et al., Heat flow and thermal history of the Anadarko Basin, Oklahoma, AAPG Bulletin, 1998, 82(2): 291.
4. Wang Jun, Wang Ji'an, Shen Jiying et al., The terrestrial heat flow in the Tarim Basin, Earth Science Bulletin (in Chinese), 1995, 20(4): 399.
5. Editorial Group of Xinjiang Petroleum Geology Record, Junggar Basin in Xinjiang Oil and Gas Region (in Chinese), Beijing: Petroleum Industry Publishing House, 1993, 99—102.
6. He Dengfa, Zhao Wenzhi, The Dynamic Evolution of Sedimentary Basin and Their Petroleum System Cycle, Beijing: Petroleum Industry Publishing House, 1999, 14—21.
7. Turcotte, D. L., Schuber, G., Geodynamics——Application of Continuum Physics to Geological Problems, New York: John Wiley & Sons, 1982, 134—195.

(Received March 30, 2000)